

## Improvement in Phosphorescence Efficiency through Tuning of Coordination Geometry of Tridentate Cyclometalated Platinum(II) Complexes

Deepak Ravindranathan,<sup>†</sup> Dileep A. K. Vezzu,<sup>†</sup> Libero Bartolotti,<sup>†</sup> Paul D. Boyle,<sup>‡</sup> and Shouquan Huo<sup>\*†</sup>

<sup>†</sup>Department of Chemistry, East Carolina University, Greenville, North Carolina 27858, and

<sup>‡</sup>Department of Chemistry, North Carolina State University, Raleigh, North Carolina 27695

Received June 1, 2010

A series of tridentate cyclometalated platinum(II) complexes (C<sup>^</sup>N<sup>\*</sup>N)PtL (L = Cl or acetylide) featuring a fused five-six-membered metallacycle were synthesized. The structure of the complexes was confirmed by X-ray crystallography. In contrast to the C<sup>^</sup>N<sup>^</sup>N platinum complexes with a fused five-five-membered metallacycle, the platinum coordination in C<sup>^</sup>N<sup>\*</sup>N complexes is much closer to a square planar geometry. The photophysical properties of the complexes were studied. The geometrical change from C<sup>^</sup>N<sup>^</sup>N to C<sup>^</sup>N<sup>\*</sup>N led to a substantial improvement in phosphorescence efficiency of the complexes with an acetylide ligand in solution at room temperature. For example, the quantum yield of (C<sup>^</sup>N<sup>\*</sup>N)PtCCPh was measured to be 56%, demonstrating a big jump from 4% reported for (C<sup>^</sup>N<sup>^</sup>N)PtCCPh.

### Introduction

Phosphorescent platinum complexes have recently attracted a great deal of attention because of their potential applications in various areas from organic electronics<sup>1</sup> to biological applications.<sup>2</sup> A key factor in the development of phosphorescent materials is the emission quantum efficiency. Geometrical and electronic optimizations have been performed to enhance the phosphorescence of platinum complexes.<sup>3</sup> For example, the use of cyclometalating ligands can induce larger d orbital splitting and reduce the possibility of nonradiative d-d transition as

demonstrated by the room temperature emission from *cis*-Pt(thpy)<sub>2</sub> (Hthpy = 2-(2-thienyl)pyridine)<sup>4a–c</sup> and (ppy)Pt(acac) (Hppy = 2-phenylpyridine).<sup>4d</sup> The development of highly efficient tridentate N<sup>^</sup>C<sup>^</sup>N (based on 1,3-dipyridylbenzene) platinum complexes<sup>5</sup> represents an effective geometrical switch from weakly emissive C<sup>^</sup>N<sup>^</sup>N (based on 6-phenyl-2,2'-bipyridine) cyclometalated platinum complexes.<sup>6</sup> A high quantum yield of 60% in dichloromethane was reported for the N<sup>^</sup>C<sup>^</sup>N platinum complex derived from 1,3-dipyridylbenzene.<sup>5b</sup> The use of N<sup>^</sup>C<sup>^</sup>N platinum complexes as highly efficient triplet emitters in organic light emitting diode (OLED) devices has been demonstrated.<sup>5f–i</sup> However, a further modification on the N<sup>^</sup>C<sup>^</sup>N platinum complex by designing a fused six-six-membered metallacycle led to a very low quantum yield (1.6%).<sup>7</sup> On the other hand, the room temperature emission quantum efficiency of [Ru(N<sup>^</sup>N<sup>^</sup>N)<sub>2</sub>]<sup>2+</sup> complexes could be

\*Author to whom correspondence should be addressed. E-mail: huos@ecu.edu.

(1) For recent reviews on OLED applications, see (a) Williams, J. A. G.; Develay, S. D.; Rochester, D. L.; Murhy, L. *Coord. Chem. Rev.* 2008, 252, 2596–2611. (b) Xiang, H.-F.; Lai, S.-W.; Lai, P. T.; Che, C.-M. Phosphorescent platinum(II) materials for OLED applications. In *Highly Efficient OLEDs with Phosphorescent Materials*; Yersin, H., Ed.; Wiley-VCH: Weinheim, 2008.

(2) (a) Siu, P. K.-M.; Ma, D.-L.; Che, C.-M. *Chem. Commun.* 2005, 1025–1027. (b) Botchway, S. W.; Charnley, M.; Haycock, J. W.; Parker, A. W.; Rochetser, D. L.; Weinstein, J. A.; Williams, J. A. G. *Proc. Natl. Acad. Sci. U.S.A.* 2008, 105, 16071–16076. (c) Ma, D.-L.; Che, C.-M.; Yan, S.-C. *J. Am. Chem. Soc.* 2009, 131, 1835–1846. (d) Wu, P.; Wong, E.L.-M.; Ma, D.-L.; Tong, G. S.-M.; Ng, K.-M.; Che, C.-M. *Chem.—Eur. J.* 2009, 15, 3652–3656.

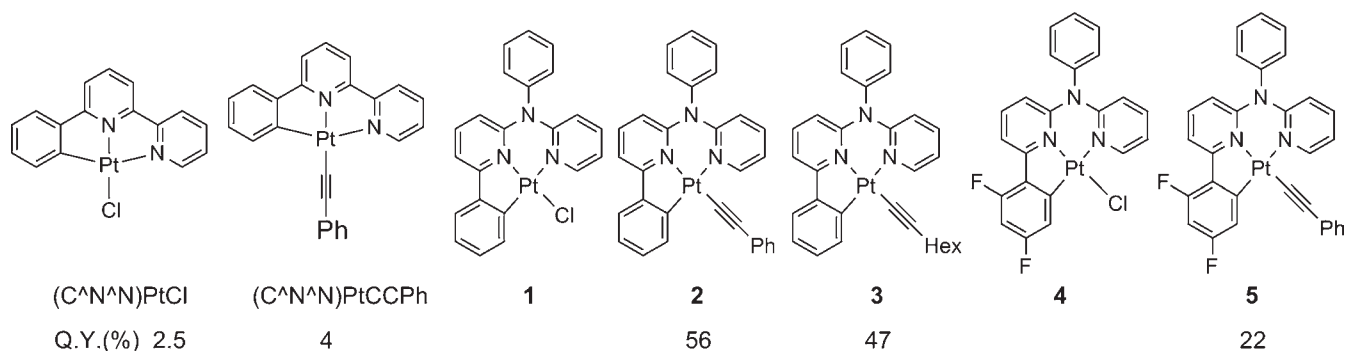
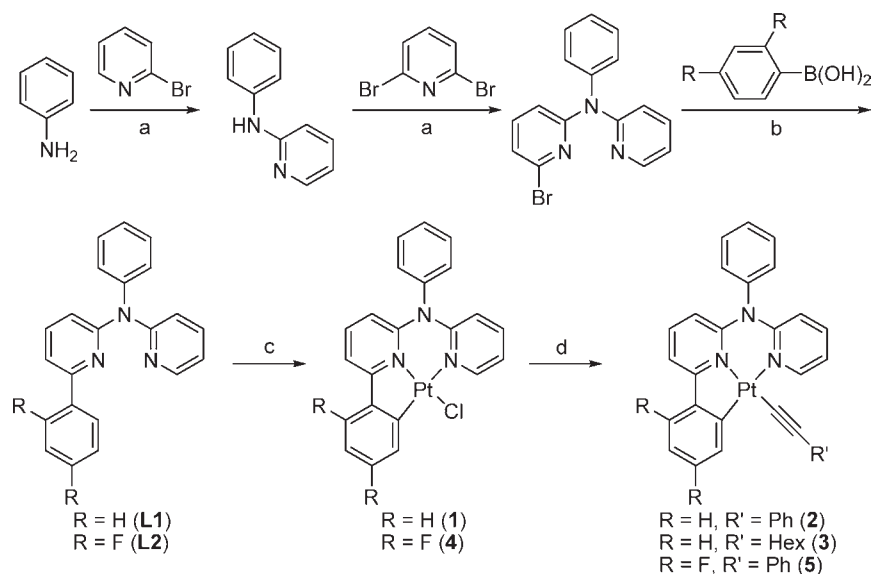
(3) (a) Chan, C.-W.; Cheng, L.-K.; Che, C.-M. *Coord. Chem. Rev.* 1994, 132, 87–97. (b) Lai, S.-W.; Che, C.-M. *Top. Curr. Chem.* 2004, 241, 27–63. (c) Yam, V. W.-W.; Wong, K. M.-C. *Top. Curr. Chem.* 2005, 257, 1–32. (d) Castellano, F. N.; Pomestchenko, I. E.; Shikhova, E.; Hua, F.; Muro, M. L.; Rajapakse, N. *Coord. Chem. Rev.* 2006, 250, 1819–1828. (e) Williams, J. A. G. *Top. Curr. Chem.* 2007, 281, 205–268. (f) Wong, K. M.-C.; Yam, V. W.-W. *Coord. Chem. Rev.* 2007, 251, 2477–2488.

(4) (a) Maestri, M.; Sandrini, D.; Balzani, V.; Chassot, L.; Jolliet, P.; von Zelewsky, A. *Chem. Phys. Lett.* 1985, 122, 375–379. (b) Maestri, M.; Sandrini, D.; Balzani, V.; von Zelewsky, A.; Jolliet, P. *Helv. Chim. Acta* 1988, 71, 134–139. (c) Deuschel-Cornioley, C.; Luond, R.; von Zelewsky, A. *Helv. Chim. Acta* 1989, 72, 377–382. (d) Brooks, J.; Babayan, Y.; Lamansky, S.; Djurovich, P. I.; Tsyba, I.; Bau, R.; Thompson, M. E. *Inorg. Chem.* 2002, 41, 3055–3066.

(5) (a) Cárdenas, D. J.; Echavarren, A. M.; Ramírez de Arellano, M. C. *Organometallics* 1999, 18, 3337–3341. (b) Williams, J. A. G.; Beeby, A.; Davies, E. S.; Weinstein, J. A.; Wilson, C. *Inorg. Chem.* 2003, 42, 8609–8611. (c) Farley, S. J.; Rochester, D. L.; Thompson, A. L.; Howard, J. A. K.; Williams, J. A. G. *Inorg. Chem.* 2005, 44, 9690–9703. (d) Develay, S.; Blackburn, O.; Thompson, A. L.; Williams, J. A. G. *Inorg. Chem.* 2008, 47, 11129–11142. (e) Rochester, D. L.; Develay, S.; Záliš, S.; Williams, J. A. G. *Dalton Trans.* 2009, 1728–1714. (f) Sotoyama, W.; Satoh, T.; Sawatani, N.; Inoue, H. *Appl. Phys. Lett.* 2005, 86, 153505 (1–3). (g) Huo, S.; Deaton, J. C.; Sowinski, A. F. U.S. Patent 7,029,766, April 18, 2006. (h) Cocchi, M.; Virgili, D.; Rochetser, D. L.; Williams, J. A. G. *Adv. Funct. Mater.* 2007, 17, 285–289. (i) Cocchi, M.; Virgili, D.; Rochetser, D. L.; Williams, J. A. G.; Kalinowski, J. *Appl. Phys. Lett.* 2007, 90, 163508 (1–3).

(6) (a) Constable, E. C.; Henney, R. P. G.; Leese, T. A.; Tocher, D. A. *J. Chem. Soc., Chem., Commun.* 1990, 513–515. (b) Lai, S.-W.; Chan, M. C. W.; Cheung, T.-C.; Peng, S.-M.; Che, C.-M. *Inorg. Chem.* 1999, 38, 4046–4055. (c) Che, C.-M.; Fu, W.-F.; Lai, S.-W.; Hou, Y.-J.; Liu, Y.-L. *Chem. Commun.* 2003, 118–119.

(7) Garner, K. L.; Parkes, L. F.; Piper, J. D.; Williams, J. A. G. *Inorg. Chem.* 2010, 49, 476–487.

**Chart 1.** Tridentate C<sup>^</sup>N<sup>\*</sup>N Platinum Complexes and the Quantum Yield in Dichloromethane Compared to the C<sup>^</sup>N<sup>^</sup>N Complexes**Scheme 1.** Synthesis of Tridentate Cyclometalated Platinum(II) Complexes<sup>a</sup>

<sup>a</sup> Reagents and conditions: (a) Pd(dba)<sub>2</sub> (2%), DPPF (2%), NaO<sup>t</sup>Bu (1.2 equiv), toluene, reflux. (b) Pd(OAc)<sub>2</sub> (2%), PPh<sub>3</sub> (8%), DME, 2 M K<sub>2</sub>CO<sub>3</sub> (aq), reflux. (c) K<sub>2</sub>PtCl<sub>4</sub> (1 equiv), AcOH, reflux. (d) alkyne, CuI, triethylamine, dichloromethane, room temperature.

improved (up to 7%) by introducing a fused six-six-membered metallacycle.<sup>8</sup>

The phosphorescence efficiency of C<sup>^</sup>N<sup>^</sup>N type of cyclometalated platinum complexes has been reported to be generally low<sup>6,9</sup> (< 10%) with only a few exceptions.<sup>10</sup> For example, the quantum yield of (C<sup>^</sup>N<sup>^</sup>N)PtCl (Chart 1) was reported to be 2.5%.<sup>6b</sup> Replacing the chloride with a phenylacetylide ((C<sup>^</sup>N<sup>^</sup>N)PtCCPh, CCPh = phenylacetylide) did not lead to much improvement in quantum yield (4%).<sup>9a</sup>

Recently, we have reported highly phosphorescent tetradentate C<sup>^</sup>N<sup>\*</sup>N<sup>^</sup>C and N<sup>^</sup>C<sup>\*</sup>C<sup>^</sup>N platinum complexes with a

fused five-six-five-membered metallacycle, where an “X<sup>^</sup>Y” (X, Y = C or N) denotes a bidentate coordination to the platinum to form a five-membered metallacycle and “X<sup>\*</sup>Y” denotes a coordination to form a six-membered metallacycle.<sup>11</sup> Compared with the tridentate C<sup>^</sup>N<sup>^</sup>N or N<sup>^</sup>C<sup>^</sup>N platinum complexes, the platinum in the tetradentate complexes displayed a coordination closer to a square planar geometry, while the tridentate C<sup>^</sup>N<sup>^</sup>N or N<sup>^</sup>C<sup>^</sup>N complexes displayed a planar but significantly distorted square geometry because of the strained fused five-five-membered chelation. Herein reported are a series of highly luminescent tridentate cyclometalated platinum complexes featuring a fused five-six-membered metallacycle, (C<sup>^</sup>N<sup>\*</sup>N)PtL (L = Cl, acetylide).

## Results and Discussion

The newly designed C<sup>^</sup>N<sup>\*</sup>N complexes **1–5** are shown in Chart 1. All complexes are strongly emissive in the solid state. Compounds **2**, **3**, and **5** are highly emissive in solution at room temperature, and the quantum yields are compared with that of the C<sup>^</sup>N<sup>^</sup>N platinum complex as shown in

(8) (a) Abrahamsson, M.; Jäger, M.; Kumar, R. J.; Österman, T.; Eriksson, L.; Persson, P.; Becker, H.-C.; Johansson, O.; Hammarström, L. *J. Am. Chem. Soc.* **2006**, *128*, 12616–12617. (b) Abrahamsson, M.; Jäger, M.; Kumar, R. J.; Österman, T.; Persson, P.; Becker, H.-C.; Johansson, O.; Hammarström, L. *J. Am. Chem. Soc.* **2008**, *130*, 15533–15542.

(9) (a) Lu, W.; Mi, B.-X.; Chan, M. C. W.; Hui, Z.; Che, C.-M.; Zhu, N.; Lee, S. T. *J. Am. Chem. Soc.* **2004**, *126*, 4958–4971. (b) Lanoë, P.-H.; Fillaut, J.-L.; Toupet, L.; Williams, J. A. G.; Bozec, H. L.; Guerchais, V. *Chem. Commun.* **2008**, 4333–4335. (c) Schneider, J.; Du, P.; Wang, X.; Brennessel, W. W.; Eisenberg, R. *Inorg. Chem.* **2009**, *48*, 1498–1506. (d) Schneider, J.; Du, P.; Jarosz, P.; Lazarides, T.; Wang, X.; Brennessel, W. W.; Eisenberg, R. *Inorg. Chem.* **2009**, *48*, 4306–4316.

(10) Kui, S. C.; Sham, I. H. T.; Cheung, C. C. C.; Ma, C.-W.; Yan, B.; Zhu, N.; Che, C.-M.; Fu, W.-F. *Chem.—Eur. J.* **2007**, *13*, 417–435.

(11) Vezzu, D. A. K.; Deaton, J. C.; Jones, J. S.; Bartolotti, L.; Harris, C. F.; Marchetti, A. P.; Kondakova, M.; Pike, R. D.; Huo, S. *Inorg. Chem.* **2010**, *49*, 5107–5119.

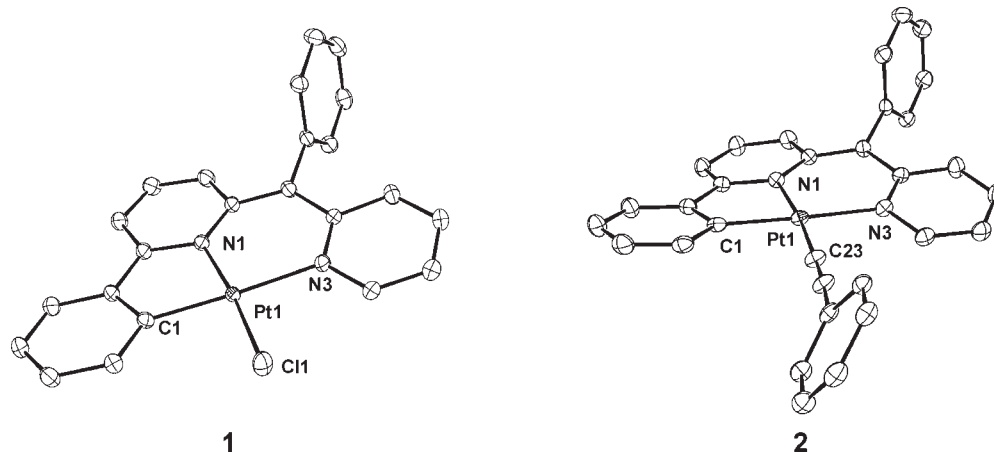


**Figure 1.** ORTEP drawing of **1** and **2**. Ellipsoids are at the 50% probability level and hydrogen atoms were omitted for clarity.

**Table 1.** Selected Bond Lengths (Å) and Angles (deg) for **1** and **2**

| complex 1  |            | complex 2  |            |
|------------|------------|------------|------------|
| Pt1–C1     | 1.9856(16) | Pt1–C1     | 1.9834(19) |
| Pt1–N1     | 1.9995(14) | Pt1–N1     | 2.0397(14) |
| Pt1–N3     | 2.1181(14) | Pt1–N3     | 2.1050(16) |
| Pt1–Cl1    | 2.3029(4)  | Pt1–C23    | 1.9594(18) |
| N2–C11     | 1.396(2)   | N2–C11     | 1.405(2)   |
| N2–C12     | 1.413(2)   | N2–C12     | 1.409(2)   |
| N2–C17     | 1.459(2)   | N2–C17     | 1.461(2)   |
| C1–Pt1–N1  | 82.80(6)   | C23–Pt1–C1 | 91.62(8)   |
| C1–Pt1–N3  | 174.82(6)  | C23–Pt1–N1 | 174.08(7)  |
| N1–Pt1–N3  | 92.12(5)   | C1–Pt1–N1  | 82.46(7)   |
| C1–Pt1–Cl1 | 91.44(5)   | C23–Pt1–N3 | 95.02(7)   |
| N1–Pt1–Cl1 | 174.22(4)  | C1–Pt1–N3  | 173.18(6)  |
| N3–Pt1–Cl1 | 93.65(4)   | N1–Pt1–N3  | 90.89(6)   |

Chart 1. As shown in Chart 1, a geometrical change from the fused five-five-membered to five-six-membered metallacycle has profound effects on the phosphorescence efficiency. It should be mentioned that a terpyridine-like ligand involving a five-six-membered chelation has been used to make luminescent platinum complexes, although the quantum yields remained low (0.2% in dichloromethane).<sup>12</sup> The low quantum yield might be attributed to the lack of a strong ligand field effect induced by the cyclometalating ligand and the acetylide present in **2**, **3**, and **5**.

**Synthesis.** The synthesis of the complexes is shown in Scheme 1. The C<sup>^</sup>N<sup>^</sup>N ligands **L1** and **L2** were prepared by three steps of Pd-catalyzed cross-coupling reactions. The C–N coupling<sup>13</sup> of aniline with 2-bromopyridine produced *N*-phenylpyridin-2-amine, which cross coupled with 2,6-dibromopyridine under the same reaction conditions to give the bromide intermediate, 6-bromo-*N*-phenyl-*N*-(pyridin-2-yl)pyridin-2-amine. The tridentate cyclometalating ligands **L1** and **L2** were then prepared in good yields by the Pd-catalyzed C–C cross coupling<sup>14</sup> of the bromide intermediate with phenylboronic acid and 2,4-difluorophenylboronic acid, respectively. The reaction of the ligands **L1** and **L2** with K<sub>2</sub>PtCl<sub>4</sub> in acetic acid gave the desired cyclometalated platinum complexes **1** and **4** in high yields. The acetylide complexes **2**, **3**, and **5** were prepared by treating **1** and **4** with

alkynes in the presence of CuI and triethylamine.<sup>9a</sup> All new compounds were characterized by <sup>1</sup>H and <sup>13</sup>C NMR, MS, and elemental analysis.

**X-ray Crystal Structure.** The molecular structure of the new complexes was confirmed by X-ray crystal structure determination of compounds **1** and **2** (Figure 1). The crystal data and structure refinement details are provided in Supporting Information (Table S1), and selected bond lengths and angles are listed in Table 1. The four angles around the platinum range from 82° to 95° with the sum of 360°, indicating planar coordination geometry. Trans C(1)–Pt(1)–N(3) angle is 174.82 (6)° and 173.18 (6)° for **1** and **2**, respectively, while the trans C–Pt–N angles in (C<sup>^</sup>N<sup>^</sup>N)PtCl<sup>6a</sup> and (C<sup>^</sup>N<sup>^</sup>N)PtCCPh<sup>9a</sup> were 160.2(9)° and 160.5(8)°, respectively, and similar angles have been reported for other platinum complexes with a fused five-five-membered metallacycle.<sup>5b</sup> As expected, the complexes with a fused five-six-membered metallacycle have a platinum coordination geometry much closer to a square. The Pt(1)–C(1) bond lengths for **1** (1.986(2) Å) and **2** (1.983(2) Å) are almost identical, which are similar to those found in the C<sup>^</sup>N<sup>^</sup>N platinum complexes.<sup>6,9</sup> The Pt(1)–N(3) bond (2.118(1) Å) that is trans to the Pt(1)–C(1) bond is longer than the Pt(1)–N(1) bond (1.999(1) Å) in **1**, which can be attributed to the trans effect of the carbon donor. The Pt(1)–C(23) bond in **2** is 1.959 (2) Å. The phenyl group of the acetylide in **2** is twisted from the platinum coordination plane. The N-phenyl group is nearly perpendicular to the coordination plane.

**DFT Calculations.** Density functional theory (DFT) calculations were performed on the compounds **1**, **2**, **4**, and **5** to examine the electronic character of the complexes. The selected molecular orbital energies and the contribution of platinum to the MOs are provided in Supporting Information (Table S2). The orbital density for the HOMOs and LUMOs is depicted in Figure 2. The HOMO of **1** is localized mainly on the platinum metal (54%) and the rest on the chlorine (10%) and the phenylpyridine group, while the HOMO of **4** is localized mainly on the platinum (54%) and chlorine atoms (17%). The contribution from the fluorine-substituted phenyl ring is negligible. On the other hand, the HOMOs of the acetylide complexes **2** and **5** are localized on the platinum (26–27%) and the triple bond (34%). The LUMOs of all the compounds are mainly localized on the phenylpyridine ring and more concentrated in the pyridine ring (60–63%).

(12) Hu, Y.-Z.; Wilson, M. H.; Zong, R.; Bonnefous, C.; McMillin, D. R.; Thummel, R. P. *Dalton Trans.* **2005**, 354–358.

(13) Yang, J.-S.; Lin, Y.-H.; Yang, C.-S. *Org. Lett.* **2002**, *4*, 777–780.

(14) Lohse, O.; Thevenin, P.; Waldvogel, E. *Synlett* **1999**, 45–48.

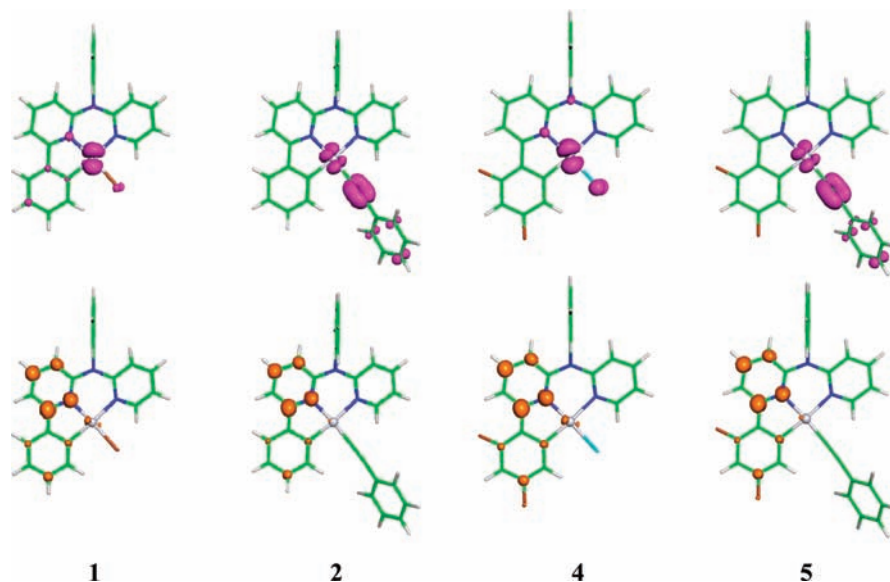


**Figure 2.** Calculated orbital density for the HOMOs (top) and LUMOs (bottom) of **1**, **2**, **4**, and **5**.

**Table 2.** Photophysical Data for Complexes **1–5**

| complex  | $\lambda_{\text{abs}}/\text{nm}^a$ ( $\epsilon \times 10^3 \text{ M}^{-1} \text{ cm}^{-1}$ ) | 298 K <sup>a</sup>              |                      |          | 77 K <sup>b</sup>               |                    | solid <sup>c</sup> $\lambda_{\text{em}}/\text{nm}$ ( $\tau/\mu\text{s}$ ) |
|----------|----------------------------------------------------------------------------------------------|---------------------------------|----------------------|----------|---------------------------------|--------------------|---------------------------------------------------------------------------|
|          |                                                                                              | $\lambda_{\text{em}}/\text{nm}$ | $\tau/\mu\text{s}^d$ | $\phi^e$ | $\lambda_{\text{em}}/\text{nm}$ | $\tau/\mu\text{s}$ |                                                                           |
| <b>1</b> | 330 (18.8), 345 (18.6), 372 (9.42)                                                           | 491, 529, 561                   | 30                   |          | 491, 529, 561                   | 30                 | 506 (12.2), 537 (12.7), 570 (12.8)                                        |
| <b>2</b> | 332 (14.4), 347 (13.8), 378 (8.87)                                                           | 495, 531                        | 9.2                  | 56       | 488, 526, 558                   | 23                 | 492 (10.7), 527 (10.9), 562 (10.9)                                        |
| <b>3</b> | 333 (17.9), 346 (17.4), 379 (9.07)                                                           | 495, 532                        | 9.7                  | 47       | 489, 527, 559                   | 21.3               | 501 (10.3), 525 (10.6), 560 (10.0)                                        |
| <b>4</b> | 324 (12.7), 343 (12.7), 369 (7.56)                                                           | 475, 512, 542                   | 35.8                 |          | 475, 512, 542                   | 35.8               | 485 (9.7), 539 (15.4), 581 (16.4)                                         |
| <b>5</b> | 327 (14.7), 345 (13.3), 373 (9.47)                                                           | 480, 514                        | 3.3                  | 22       | 473, 508, 538                   | 27.4               | 482 (9.8), 531 (16.0), 568 (16.2)                                         |

<sup>a</sup> Measurements were carried out in a solution of dichloromethane. <sup>b</sup> Measurements were carried out in a solution of 2-methyltetrahydrofuran. <sup>c</sup> Solid state studies were measured with pure powder samples. <sup>d</sup> Measured in deoxygenated dichloromethane. <sup>e</sup> Quantum yields were measured in deoxygenated dichloromethane with a deoxygenated solution of (N<sup>^C^N</sup>)PtCl<sup>5b</sup> in dichloromethane ( $\phi = 60$ ) as the reference.

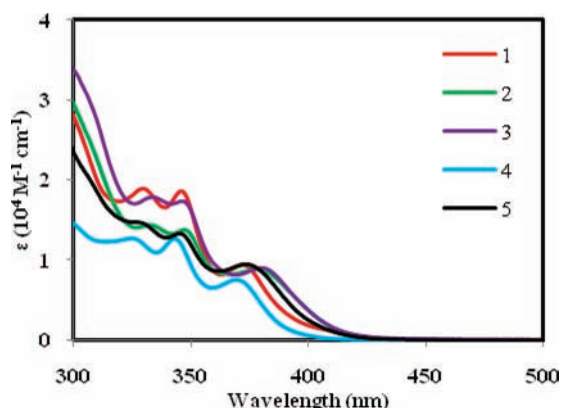


**Figure 3.** Absorption spectra of **1–5** in dichloromethane.

**Photophysical Properties.** Photophysical data are summarized in Table 2. The absorption spectra of **1–5** are shown in Figure 3. The emission spectra of **1–5** in frozen glass are shown in Figure 4 and those of **2**, **3**, and **5** in dichloromethane solution in Figure 5. For comparison, the absorption, fluorescence emission, and phosphorescence emission spectra of the ligands **L1** and **L2** were recorded and provided in Supporting Information (Figure S1). The assignment of absorption spectra of the complexes can be made by analogy with other cyclometalated platinum complexes. High energy bands with stronger absorbance can be

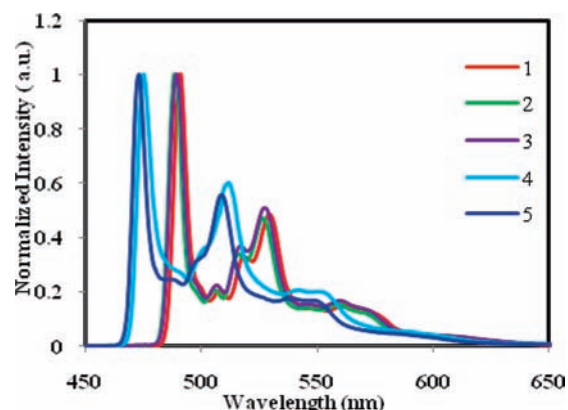


**Figure 4.** Normalized emission spectra of complex **1–5** in 2-methyltetrahydrofuran (77 K).  $\lambda_{\text{ex}} = 350 \text{ nm}$ .

assigned as ligand based  $^1\pi-\pi^*$  transitions, while the low energy absorptions that were not presented in the absorption spectra of the corresponding ligands can be assigned as charge transfer bands. The lowest charge transfer bands may be assigned as mixed MLCT/LLCT/ILCT (**1**) or MLCT/LLCT transitions (**2–5**) based on the HOMO and LUMO characters of the complexes. The solvent effect was found to be moderate on the lowest absorption band for **1** and **2** (Supporting Information, Tables S3 and S4). The fluorine substituent caused blue shift of electronic spectra as observed in other complexes.<sup>4d,11</sup>



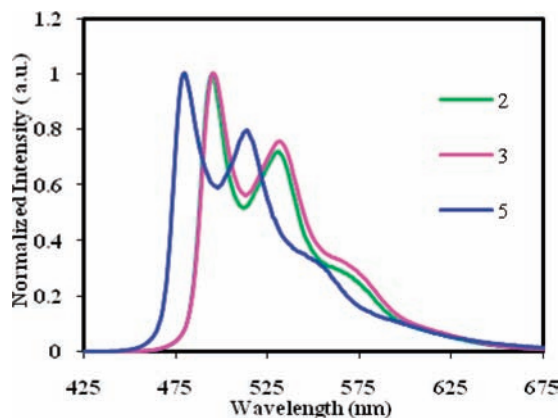


**Figure 5.** Emission spectra of **2**, **3**, and **5** in dichloromethane at room temperature.  $\lambda_{\text{ex}} = 350$  nm.

All new complexes are emissive in frozen glass. The spectra in frozen glass are highly structured (Figure 4) and display a vibronic progression of  $1450\text{--}1520\text{ cm}^{-1}$  that is the typical range of aromatic ring stretching. The emissions in frozen glass of 2-MeTHF have lifetimes in the range of  $21.3\text{--}35.8\ \mu\text{s}$ . These features suggest that the emissions are based on ligand-centered triplet transitions. All three complexes **1–3** derived from the ligand **L1** display identical band shape and have nearly the same energy, indicating that the emissions may originate from similar ligand-centered excited states. Compared with the phosphorescence of ligand **L1** (see Supporting Information, Figure S1), the emissions of the complexes are red-shifted, which has also been observed in other cyclometalated platinum complexes.<sup>4</sup> The complexes **4** and **5** exhibit a spectroscopic characteristic similar to those of **1–3** except for the blue shift of the emission energy. Complexes **1–5** also emit intensely in solid state. The emission spectra obtained with pure powder sample are provided in Supporting Information (Figures S2 and S3).

In dichloromethane at room temperature, the emissions of compounds **1** and **4** were very weak and the quantum yields were not estimated. However, when the chloride was replaced with an acetylide, the resulted complexes **2**, **3**, and **5** emitted intensely in dichloromethane (Figure 5). This may be due to the stronger acetylide ligands, which further raise the energy of nonradiative d-d transitions. Distortion of the triplet states may not be responsible for the difference in emission efficiency between **1** and **2**, since the compound **2** has more distorted triplet geometry compared to the ground state (Supporting Information, Figure S4). Given the fact that at 77 K both the chloride and acetylide complexes emitted intensely and displayed essentially same emission spectra, the lack of room temperature emission of the chloride complexes in solution might be due to thermally accessible nonemissive metal-centered transitions.

The quantum yield of 56% measured for compound **2** represents a significant improvement when compared with 4% of  $(\text{C}^{\wedge}\text{N}^{\wedge}\text{N})\text{PtCCPh}$ . Such a jump in quantum yield is quite remarkable, since the geometric change from  $\text{C}^{\wedge}\text{N}^{\wedge}\text{N}$  to  $\text{C}^{\wedge}\text{N}^{\wedge}\text{N}$  does not seem to increase the rigidity of the molecule. Possibly, the  $\text{C}^{\wedge}\text{N}^{\wedge}\text{N}$  ligand exerted a stronger field as the square geometry was restored in the  $\text{C}^{\wedge}\text{N}^{\wedge}\text{N}$  platinum complexes. Concentration quenching was not observed since the lifetimes of the emission

remained largely unchanged as the concentration of the complexes increased from  $1 \times 10^{-6}$  M to  $1 \times 10^{-4}$  M. The perpendicular N-phenyl ring and the twisted acetylide groups may prevent any Pt–Pt or  $\pi\text{--}\pi$  interactions that are considered to be the main cause of self-quenching in square planar platinum complexes, which might be another factor contributing to the high quantum efficiency. Solvent effect on the emission of **1** and **2** was small (Supporting Information, Table S3 and S4). The emission spectra of **2**, **3**, and **5** displayed vibrational side bands. The lifetimes of the emission of **2** and **3** are nearly the same ( $9.2$  and  $9.7\ \mu\text{s}$ , respectively), while the emission of **5** has a much shorter lifetime of  $3.3\ \mu\text{s}$ . The radiative decay rates constant estimated from the quantum yield and lifetimes for **2**, **3**, and **5** were  $6.1$ ,  $4.9$ , and  $6.7 \times 10^4\ \text{s}^{-1}$ , respectively. The sum of nonradiative decay rate constants for **2**, **3**, and **5** were estimated to be  $4.8$ ,  $5.5$ , and  $23.6 \times 10^4\ \text{s}^{-1}$ , respectively. The lower quantum efficiency observed for **5** can be attributed to the faster nonradiative decay (4 times faster than those for **2** and **3**), although such nonradiative pathways are not clear. In contrast, the nonradiative decay reported for the  $(\text{C}^{\wedge}\text{N}^{\wedge}\text{N})\text{PtCCPh}$  ( $2.5 \times 10^6\ \text{s}^{-1}$ )<sup>9a</sup> is much faster. Further studies may be required for unveiling other factors that affect the phosphorescence efficiency.<sup>15</sup> The emission features of **2**, **3**, and **5** including lifetimes and the spectral band shape suggest a ligand-centered emission with MLCT admixture in dichloromethane at ambient temperature.

In summary, we have demonstrated that, by tuning coordination geometry of tridentate cyclometalated platinum complexes from a fused five–five-membered metallacycle to the five–six-membered metallacycle that is closer to ideal square planar geometry, a substantial increase in emission quantum efficiency could be achieved. Since other similar geometrical variations such as  $(\text{N}^{\wedge}\text{N}^{\wedge}\text{C})\text{PtL}$ ,  $(\text{N}^{\wedge}\text{C}^{\wedge}\text{N})\text{PtL}$ , and  $(\text{C}^{\wedge}\text{N}^{\wedge}\text{C})\text{PtL}$  can be envisaged for tridentate complexes and the ligand design and synthesis exemplified in this report is representative of simplicity and modularity (Scheme 1), this study should open a new avenue to a large number of highly luminescent platinum complexes potentially useful for various applications as mentioned before. Currently, we are working on the  $\text{N}^{\wedge}\text{N}^{\wedge}\text{C}$  and  $\text{N}^{\wedge}\text{C}^{\wedge}\text{N}$  platinum complexes and the results will be reported in due course.

## Experimental Section

**Synthesis.** All reactions involving moisture- and/or oxygen-sensitive organometallic complexes were carried out under nitrogen atmosphere and anhydrous conditions. Tetrahydrofuran (THF) and 2-methyltetrahydrofuran were distilled from sodium and benzophenone under nitrogen before use. All other anhydrous solvents were purchased from Aldrich Chemical Co. and were used as received. All other reagents were purchased from chemical companies and were used as received. Mass spectra were measured on a Waters spectrometer. NMR spectra were measured on a Mercury VX 300 or a Varian 500 spectrometer. Spectra were taken in  $\text{CDCl}_3$  or  $\text{CD}_2\text{Cl}_2$  using tetramethylsilane as standard for  $^1\text{H}$  NMR chemical shifts and the solvent peak ( $\text{CDCl}_3$ , 77.0 ppm;  $\text{CD}_2\text{Cl}_2$ , 53.8 ppm) as standard for  $^{13}\text{C}$  NMR chemical shifts. Elemental analyses were performed at Atlantic Microlab, Inc. in Norcross, Georgia.

(15) (a) Tong, G.-M.; Che, C.-M. *Chem.—Eur. J.* **2009**, *15*, 7225–7237. (b) Ma, B.; Djurovich, P. I.; Thompson, M. E. *Coord. Chem. Rev.* **2005**, *249*, 1501–1510.

**Preparation of *N*-Phenylpyridin-2-amine<sup>16</sup>.** **General Procedure.** To a 250 mL dry, nitrogen flushed flask were charged 2-bromopyridine (3.16 g, 20 mmol), sodium *tert*-butoxide (2.31 g, 24 mmol), Pd(dba)<sub>2</sub> (0.46 g, 0.8 mmol), DPPF (0.44 g, 0.8 mmol), aniline (2.73 mL, 30 mmol), and anhydrous toluene (75 mL). The mixture was refluxed for 24 h. After cooling to room temperature, 50 mL of ethyl acetate was added and stirred for a while. The precipitate formed was filtered and the filtrate was evaporated. The crude mixture was purified by chromatography on silica gel with pure dichloromethane first to remove excess aniline and then a mixture of dichloromethane and ethyl acetate (v/v = 10:1) and recrystallization from hexane and dichloromethane to provide white crystals. 2.16 g, yield 89%.

**6-Bromo-*N*-phenyl-*N*-(pyridin-2-yl)pyridin-2-amine.** This compound was prepared from *N*-phenylpyridin-2-amine and 2,6-dibromopyridine following the general procedure described above and purified by chromatography on silica gel with a mixture of hexane and ethyl acetate (v/v = 5:1), light brown solid, 1.16 g, 89%. <sup>1</sup>H NMR (500 MHz, CDCl<sub>3</sub>) δ 8.31 (ddd, *J* = 5 Hz, 2 Hz, 1 Hz, 1H), 7.58 (dt, *J* = 7.5 Hz, 2 Hz, 1H), 7.38 (t, *J* = 7.5 Hz, 2H), 7.33 (t, *J* = 7.5 Hz, 1H), 7.27–7.23 (m, 1H), 7.22–7.18 (m, 2H), 7.11 (d, *J* = 7.5 Hz, 1H), 7.05 (d, *J* = 8 Hz, 1H), 6.96–6.94 (m, 1H), 6.79 (d, *J* = 8.5 Hz, 1H); <sup>13</sup>C NMR (75 MHz, CDCl<sub>3</sub>) δ 157.86, 157.35, 148.29, 144.19, 139.70, 139.31, 137.47, 129.73, 127.56, 126.14, 121.19, 118.76, 117.53, 114.08. MS: *m/z* calcd for C<sub>16</sub>H<sub>12</sub>N<sub>3</sub>Br: 325.02. Found 326.07 (M+H<sup>+</sup>). Anal. Calcd for C<sub>16</sub>H<sub>12</sub>N<sub>3</sub>Br: C, 58.91; H, 3.71; N, 12.88. Found C, 59.42; H, 3.72; N, 12.73.

**Preparation of Ligand L1. Representative Procedure.** To a 25 mL dry, nitrogen flushed flask were charged 6-bromo-*N*-phenyl-*N*-(pyridin-2-yl)pyridin-2-amine (652 mg, 2 mmol), phenylboronic acid (292 mg, 2.4 mmol), triphenylphosphine (42 mg, 0.16 mmol), and DME (7 mL). A homogeneous solution was formed. To this solution was added 2 M K<sub>2</sub>CO<sub>3</sub> (2.5 mL, 5 mmol). After the mixture was purged with nitrogen, Pd(OAc)<sub>2</sub> (8.9 mg, 0.04 mmol) was added. The mixture was refluxed for 6 h then cooled to room temperature. After cooling to room temperature, 15 mL of ethyl acetate was added and stirred for a while. The precipitate formed was filtered and the filtrate was transferred into a separating funnel and the organic layer was separated and retained. The aqueous phase was extracted with ethyl acetate (3 × 25 mL). The combined organic layers were washed with water (50 mL) and brine (50 mL) and dried over MgSO<sub>4</sub>. Filtration and evaporation produced dark brown oil, which was purified by chromatography on silica gel with a mixture of hexane and ethyl acetate (v/v = 3:1) and recrystallization from hexane and dichloromethane to provide white crystals, 340 mg, yield 54%. <sup>1</sup>H NMR (500 MHz, CDCl<sub>3</sub>) δ 8.34 (dd, *J* = 5 Hz, 2 Hz, 1H), 7.84–7.82 (m, 2H), 7.61–7.55 (m, 2H), 7.41–7.32 (m, 5H), 7.27–7.22 (m, 4H), 7.18 (d, *J* = 8.5 Hz, 1H), 6.94–6.92 (m, 1H), 6.87 (d, *J* = 8.5 Hz, 1H); <sup>13</sup>C NMR (75 MHz, CDCl<sub>3</sub>) δ 158.04, 157.61, 155.49, 148.32, 144.91, 139.04, 138.15, 137.09, 129.51, 128.73, 128.50, 127.59, 126.64, 125.57, 117.99, 117.39, 114.46, 114.06. MS: *m/z* calcd for C<sub>22</sub>H<sub>17</sub>N<sub>3</sub>: 323.14. Found 324.17 (M+H<sup>+</sup>). Anal. Calcd for C<sub>22</sub>H<sub>17</sub>N<sub>3</sub>: C, 81.71; H, 5.30; N, 12.99. Found C, 81.91; H, 5.32; N, 13.11.

**Ligand L2.** This compound was prepared following the representative procedure, yellow solid, 0.713 g, yield 98%. <sup>1</sup>H NMR (500 MHz, CDCl<sub>3</sub>) δ 8.33 (dd, *J* = 5 Hz, 2 Hz, 1H), 7.75–7.71 (m, 1H), 7.59–7.53 (m, 2H), 7.43–7.36 (m, 3H), 7.25–7.20 (m, 3H), 7.09 (d, *J* = 8 Hz, 1H), 6.93–6.90 (m, 2H), 6.84–6.80 (m, 2H); <sup>13</sup>C NMR (75 MHz, CDCl<sub>3</sub>) δ 162.87 (dd, *J*<sub>C-F</sub> = 249.4 Hz, 12 Hz, 1C), 160.71 (dd, *J*<sub>C-F</sub> = 251.4 Hz, 12 Hz, 1C), 157.94, 157.53, 150.35 (d, *J*<sub>C-F</sub> = 3 Hz, 1C), 148.29, 144.75, 137.99, 137.19, 132.03 (dd, *J*<sub>C-F</sub> = 9.5 Hz, 4.5 Hz, 1C), 129.49, 127.44, 125.58, 123.31 (dd, *J*<sub>C-F</sub> = 11 Hz, 3.5 Hz, 1C), 118.13, 117.95, 117.27, 114.90, 11.56 (dd, *J*<sub>C-F</sub> = 20.5 Hz, 3.5

Hz, 1C), 104.05 (t, *J*<sub>C-F</sub> = 52.1 Hz, 25 Hz, 1C). MS: *m/z* calcd for C<sub>22</sub>H<sub>15</sub>N<sub>3</sub>F<sub>2</sub>: 359.12. Found 360.14 (M + H<sup>+</sup>). Anal. Calcd for C<sub>22</sub>H<sub>15</sub>N<sub>3</sub>F<sub>2</sub>: C, 73.53; H, 4.21; N, 11.69. Found C, 73.66; H, 4.11; N, 11.50.

**Preparation of Platinum Complex 1.** To a 100 mL dry, nitrogen flushed flask was charged ligand L1 (323 mg, 1 mmol), K<sub>2</sub>PtCl<sub>4</sub> (415.5 mg, 1 mmol), and glacial acetic acid (50 mL). The mixture was degassed and refluxed under nitrogen for 21 h. After cooling to room temperature, the yellow and orange precipitates were collected by filtration and washed with water, and dried in air. The crude material was purified by flash chromatography on silica gel with dichloromethane. The compound was further recrystallized from dichloromethane and hexanes to give yellow solid, 490 mg, yield 65%. <sup>1</sup>H NMR (500 MHz, CD<sub>2</sub>Cl<sub>2</sub>) δ 9.90 (dd, *J* = 6 Hz, 2 Hz, 1H), 8.13 (dd, *J* = 8 Hz, 1.5 Hz, <sup>3</sup>*J*<sub>Pt-H</sub> = 16 Hz, 1H), 7.70–7.65 (m, 4H), 7.60 (t, *J* = 7.5 Hz, 1H), 7.52 (d, *J* = 7 Hz, 1H), 7.48–7.43 (m, 3H), 7.22 (dt, *J* = 7.5 Hz, 1.5 Hz, 1H), 7.11 (t, *J* = 7.5 Hz, 1H), 7.04 (t, *J* = 6 Hz, 1H), 6.80 (d, *J* = 8.5 Hz, 1H), 6.58 (d, *J* = 8.5 Hz, 1H); <sup>13</sup>C NMR (75 MHz, CD<sub>2</sub>Cl<sub>2</sub>) δ 166.43, 150.43, 150.39, 149.12, 144.94, 142.79, 141.76, 138.08, 137.64, 135.55, 131.59, 130.75, 139.91, 129.91, 129.26, 123.92, 123.21, 118.58, 117.40, 115.56, 113.04. MS: *m/z* calcd for C<sub>24</sub>H<sub>19</sub>N<sub>4</sub>Pt (acetonitrile complex): 558.13; found 558.13; Anal. Calcd for C<sub>22</sub>H<sub>16</sub>N<sub>3</sub>ClPt: C, 47.79; H, 2.92; N, 7.60. Found C, 47.64; H, 2.92; N, 7.63.

**Preparation of Complex 2.** To a 50 mL dry, nitrogen flushed flask was charged complex 1 (100 mg, 0.18 mmol), phenylacetylene (59.5 μL, 0.54 mmol), Et<sub>3</sub>N (1.65 mL), CuI (2.8 mg), and dichloromethane (17 mL). The mixture was stirred at room temperature in the absence of light for 12 h. The reaction mixture was then evaporated and the crude product was purified by flash chromatography on silica gel with dichloromethane as eluting solvent to provide yellow crystals, 650 mg, 65%. <sup>1</sup>H NMR (500 MHz, CD<sub>2</sub>Cl<sub>2</sub>) δ 10.23 (dd, *J* = 6 Hz, 2 Hz, 1H), 8.43 (dd, *J* = 8 Hz, 1.5 Hz, <sup>3</sup>*J*<sub>Pt-H</sub> = 26 Hz, 1H), 7.78–7.65 (m, 4H), 7.63–7.60 (m, 2H), 7.53–7.51 (m, 3H), 7.45 (d, *J* = 7.5 Hz, 2H), 7.30 (t, *J* = 7.5 Hz, 2H), 7.24–7.17 (m, 2H), 7.11 (dt, *J* = 7.5 Hz, 1 Hz, 1H), 6.98 (dt, *J* = 7 Hz, 1.5 Hz, 1H), 6.75 (d, *J* = 8.5 Hz, 1H), 6.56 (d, *J* = 9 Hz, 1H); <sup>13</sup>C NMR (75 MHz, CD<sub>2</sub>Cl<sub>2</sub>) δ 165.14, 153.62, 150.97, 150.72, 145.06, 143.34, 142.77, 139.15, 138.20, 138.01, 134.12, 131.95, 131.80, 130.98, 130.11, 129.52, 128.36, 125.48, 123.71, 123.68, 118.83, 118.03, 115.08, 112.96, 105.40, 101.97. MS: *m/z* calcd for C<sub>30</sub>H<sub>21</sub>N<sub>3</sub>Pt: 618.14; found 619.17 (M + H<sup>+</sup>); Anal. Calcd for C<sub>30</sub>H<sub>21</sub>N<sub>3</sub>Pt: C, 58.25; H, 3.42; N, 6.79. Found C, 57.64; H, 3.34; N, 6.82.

**Complex 3.** This compound was prepared following the general procedure for complex 2, yellow crystals, 31% yield.

<sup>1</sup>H NMR (500 MHz, CD<sub>2</sub>Cl<sub>2</sub>) δ 10.32 (dd, *J* = 6 Hz, 2 Hz, 1H), 8.41 (dd, *J* = 7.5 Hz, 1.5 Hz, <sup>3</sup>*J*<sub>Pt-H</sub> = 27 Hz, 1H), 7.69–7.57 (m, 6H), 7.48 (d, *J* = 7.5 Hz, 1H), 7.43–7.41 (m, 2H), 7.18 (dt, *J* = 7.5 Hz, 1.5 Hz, 1H), 7.07 (dt, *J* = 7.5 Hz, 1.5 Hz, 1H), 6.93 (dt, *J* = 7 Hz, 1.5 Hz, 1H), 6.71 (d, *J* = 9 Hz, 1H), 6.52 (d, *J* = 8 Hz, 1H), 2.6 (t, *J* = 7 Hz, 2H), 1.68–1.64 (m, 2H), 1.59–1.56 (m, 2H), 1.39–1.36 (m, 4H), 0.93 (t, *J* = 7 Hz, 3H); <sup>13</sup>C NMR (75 MHz, CD<sub>2</sub>Cl<sub>2</sub>) δ 165.16, 153.70, 150.86, 150.59, 145.05, 143.38, 143.26, 139.41, 137.77, 137.71, 131.88, 130.95, 129.99, 129.71, 123.53, 123.30, 118.47, 117.85, 114.95, 112.82, 100.43, 89.04, 32.15, 31.39, 29.41, 23.19, 22.12, 14.35. MS: *m/z* calcd for C<sub>30</sub>H<sub>29</sub>N<sub>3</sub>Pt: 626.20; found 627.24 (M + H). Anal. Calcd for C<sub>30</sub>H<sub>29</sub>N<sub>3</sub>Pt: C, 57.50; H, 4.66; N, 6.71. Found C, 57.42; H, 4.59; N, 6.74.

**Complex 4.** Following the representative procedure for complex 1, this complex was prepared in 49% yield. <sup>1</sup>H NMR (500 MHz, CD<sub>2</sub>Cl<sub>2</sub>) δ 9.84 (dd, *J* = 6 Hz, 1.5 Hz, 1H), 7.84–7.82 (m, 1H), 7.75 (dd, *J* = 9 Hz, 2.5 Hz, 1H), 7.72–7.66 (m, 4H), 7.61 (t, *J* = 8 Hz, 1H), 7.48 (d, *J* = 7.5 Hz, 2H), 7.05 (dt, *J* = 7 Hz, 1 Hz, 1H), 6.85 (d, *J* = 7.5 Hz, 1H), 6.69–6.61 (m, 2H); <sup>13</sup>C NMR (75 MHz, CD<sub>2</sub>Cl<sub>2</sub>) δ 150.53, 149.58, 142.83, 138.70, 138.51, 134.13, 131.84, 130.95, 130.25, 118.97, 117.60, 117.40, 117.02, 116.74,

(16) Katritzky, A. R.; Huang, T.-B.; Voronkov, M. V. *J. Org. Chem.* **2001**, *66*, 1043–1045.

115.94, 99.91 (t,  $J_{C-F} = 54$  Hz, 27 Hz, 1C) (only partial carbon signals were observed because of very poor solubility). MS:  $m/z$  calcd for  $C_{24}H_{17}F_2N_4Pt$  (acetonitrile complex): 594.11; found 594.13; Anal. Calcd for  $C_{22}H_{14}N_3F_2ClPt$ : C, 44.34; H, 2.40; N, 7.14. Found C, 44.19; H, 2.26; N, 6.95.

**Complex 5.** This compound was prepared following the general procedure for complex **2**, yellow crystals, 82% yield.  $^1H$  NMR (500 MHz,  $CD_2Cl_2$ )  $\delta$  10.19 (dd,  $J = 6$  Hz, 2 Hz, 1H), 8.07 (dd,  $J = 9.5$  Hz, 2.5 Hz,  $^3J_{Pt-H} = 30$  Hz, 1H), 7.89 (dd,  $J = 8$  Hz, 3 Hz, 1H), 7.72–7.66 (m, 4H), 7.62 (t,  $J = 7$  Hz, 1H), 7.51 (d,  $J = 8$  Hz, 2H), 7.47 (d,  $J = 6.5$  Hz, 2H), 7.30 (t,  $J = 7.5$  Hz, 2H), 7.20 (t,  $J = 7.5$  Hz, 1H), 6.99 (dt,  $J = 7$  Hz, 1 Hz, 1H), 6.79 (d,  $J = 8.5$  Hz, 1H), 6.64–6.59 (m, 2H);  $^{13}C$  NMR (75 MHz,  $CD_2Cl_2$ )  $\delta$  162.98 (dd,  $J_{C-F} = 248.4$  Hz, 12.5 Hz, 1C), 161.33 (d,  $J_{C-F} = 7.5$  Hz, 1C), 160.24 (dd,  $J_{C-F} = 257.6$  Hz, 12.5 Hz, 1C), 153.60, 150.75, 150.53, 147.12 (d,  $J_{C-F} = 7.5$  Hz, 1C), 143.23, 138.61, 138.19, 131.92, 131.75, 131.01, 130.14, 129.15, 128.42, 125.75, 120.86, 120.65, 118.85, 118.10, 116.88, 116.58, 115.37, 105.01, 101.59, 99.52 (t,  $J_{C-F} = 54.6$  Hz, 27.5 Hz, 1C). MS:  $m/z$  calcd for  $C_{30}H_{19}N_3F_2Pt$ : 654.12; found 655.16 (M +  $H^+$ ); Anal. Calcd for  $C_{30}H_{19}N_3F_2Pt$ : C, 55.05; H, 2.93; N, 6.42. Found C, 54.78; H, 2.78; N, 6.23.

**DFT Calculations.** The electronic structure calculations were performed on complexes **1**, **2**, **4**, and **5** using DMol3,<sup>17</sup> a numerical based density functional computer program.<sup>18,19</sup> The orbitals for each atom in the molecule are represented by a double numerical plus double polarization basis set that was developed in our laboratory. For platinum, there were both f and g polarization functions. For all calculations, we used the Becke-Tsuneda-Hirao exchange-correlation energy-density functional,<sup>20,21</sup> a 20 Bohr cutoff and a fine integration grid. The SCF convergence was set to  $1.0 \times 10^{-8}$  and the geometry was considered converged when the gradient was less than  $5.0 \times 10^{-4}$  hartree/Bohr. Relativity is introduced into the calculations with the scattering theoretic approach for all electron scalar relativistic corrections introduced by Delley.<sup>22</sup> Since the experiments were performed in dichloromethane, we employed the solvation model COSMO<sup>23</sup> (with a dielectric constant of 9.08) to simulate the possible effect that solvent might have on the present calculations.

**Photophysical Experiments.** Absorption spectra were recorded on a Shimadzu 2445 UV/vis spectrophotometer, using 1 cm path-length quartz cuvettes. The steady-state emission spectra were measured using a PTI QM-4CW system and an excitation source with the spectral bandpass of 2 nm was used. Quantum yields were measured using comparative method at room temperature in a dichloromethane solution. The solution was deoxygenated by purging with argon gas for 20 min. A long necked 1 cm quartz cuvette was used for measurements. The cuvette was cooled with a dry ice-acetone bath to prevent solvent loss. A deoxygenated solution of (N<sup>^C^A^N</sup>)PtCl in dichloromethane

(Q.Y. 60%)<sup>5b</sup> was used as a reference. The optical density of both sample and reference solutions was maintained below 0.1 AU at and above the excitation wavelength. Emission spectra in a frozen glass were recorded in 2-MeTHF at 77 K. Solid-state emission spectra were recorded using a powder sample holder. Phosphorescence lifetime measurements were performed on the same fluorimeter equipped with variable high rep rate pulsed xenon source for excitation and were limited to lifetimes  $> 0.4 \mu s$ . Delayed phosphorescent emission spectra of the ligands were measured using a gated analog detector with R928 red extended PMT in 2-MeTHF at 77 K. The radiative and nonradiative rate constants were calculated from the luminescent quantum yield ( $\phi$ ) and lifetime ( $\tau$ ) of the phosphorescent complex according to eqs 1 and 2, respectively,

$$k_r = \phi\tau^{-1} \quad (1)$$

$$k_{nr} = k_r(\phi^{-1} - 1) \quad (2)$$

where  $k_r$  and  $k_{nr}$  are the radiative and nonradiative rate constant, respectively.

**X-ray Crystallography. Data Collection and Processing.** The crystals were prepared using a solvent diffusion method. The sample was mounted on a nylon loop with a small amount of Paratone N oil. All X-ray measurements were made on a Bruker-Nonius Kappa Axis X8 Apex2 diffractometer at a temperature of 110 K. The data collection strategy was a number of  $\omega$  and  $\phi$  scans. The frame integration was performed using SAINT.<sup>24</sup> The resulting raw data was scaled and absorption was corrected using a multiscan averaging of symmetry equivalent data using SADABS.<sup>25</sup> The structure was solved by direct methods using the XS program.<sup>26</sup> All non-hydrogen atoms were obtained from the initial solution. The hydrogen atoms were introduced at idealized positions and were allowed to ride on the parent atom. The structural model was fit to the data using full matrix least-squares based on  $F^2$ . The calculated structure factors included corrections for anomalous dispersion from the usual tabulation. The structure was refined using the XL program from SHELXTL,<sup>27</sup> and graphic plots were produced using the NRCVAX crystallographic program suite.

**Acknowledgment.** Financial support from ECU and the Research Corporation for Science Advancement is gratefully acknowledged. D.R. is the recipient of the undergraduate research award of ECU. P.D.B. thanks the Department of Chemistry of North Carolina State University and the State of North Carolina for funding the purchase of the Apex2 diffractometer.

**Supporting Information Available:** Crystallographic data in CIF format for **1** and **2**. DFT calculation results. Solvent effects. Electronic spectra of the ligands. Solid emission spectra and proton NMR spectra of complexes **1–5**. This material is available free of charge via the Internet at <http://pubs.acs.org>.

- (17) DMol3; Accelrys Inc.; San Diego, CA.  
 (18) (a) Delley, B. *J. Chem. Phys.* **1990**, *92*, 508–517. (b) Delley, B. *J. Chem. Phys.* **2000**, *113*, 7756–7764.  
 (19) Delley, B. DMol a Standard Tool for Density Functional Calculations: Review and Advances. In *Modern Density Functional Theory: A Tool for Chemistry*; Seminario, J. M., Politzer, P., Eds.; Elsevier Science Publishing: Amsterdam, 1995; Vol. 2.  
 (20) Becke, A. D. *J. Chem. Phys.* **1988**, *88*, 2547–2553.  
 (21) Tsuneda, T.; Suzumura, T.; Hirao, K. *J. Chem. Phys.* **1999**, *110*, 10664–10678.  
 (22) Delley, B. *Int. J. Quantum Chem.* **1998**, *69*, 423–433.  
 (23) Klamt, A.; Schuurmann, G. *J. Chem. Soc. Perkin Trans. 2* **1993**, 799–805.

- (24) Bruker-Nonius, SAINT, version 2009.9; Bruker-Nonius: Madison, WI 53711, USA, 2009.  
 (25) Bruker-Nonius, SADABS, version 2009.9; Bruker-Nonius: Madison, WI 53711, USA, 2009.  
 (26) Bruker-AXS, XS, version 2009.9; Bruker-AXS: Madison, WI 53711, USA, 2009.  
 (27) Bruker-AXS, XL, version 2009.9; Bruker-AXS, Madison, WI 53711, USA, 2009.